Synchronised Measurement Technology for Analysis of Transmission Lines Faults

Vladimir Terzija
The University of Manchester
terzija@ieee.org

Mladen Kezunovic
Texas A&M University
kezunov@mail.ece.tamu.edu

Abstract

A new numerical algorithm for the analysis of single line to ground faults on short overhead transmission lines is presented in this paper. It is based on synchronised sampling at two line terminals and an accurate fault model including the arcing phenomena and tower footing resistance at the fault point. The core of the algorithm is an efficient non-recursive parameter estimation method. A dynamic arc model is included in the fault model to represent the arc's interaction with the external network. The algorithm accurately estimates the arc voltage amplitude, tower footing resistance, and the fault location, simultaneously. The algorithm is derived in the time domain, and is based on the synchronized acquisition of currents and voltages at both line terminals. Case studies based on simulated data are presented to demonstrate the effectiveness of the new method.

1. Introduction

Fault locators determine the distance to the fault using measurements from the local line terminal(s). In modern power systems, which are designed to exploit the existing assets optimally, the importance of locating faults quickly and precisely is becoming critically important. Prompt and accurate location of the faults in a large-scale transmission system can accelerate the system restoration, reduce the outage time and improve the system reliability [1-4].

Great efforts have been made in the past developing various algorithms for improved fault location estimates [1-15]. One-terminal algorithms using the local voltages and currents are proposed in [2-3]. The accuracy of this type of algorithm is normally adversely affected by the fault resistance, and a compensation technique is proposed to alleviate this effect [3]. To improve the accuracy of estimation, the authors of [4-5] have designed special one-end algorithms applicable to the phase to ground faults. A method for parallel line fault location using one-end data is reported in [6]. Reference [7] presents an approach using the pre-fault and fault current phasors at one end of the line for estimating the fault location assuming the source impedances to be available. Fault location techniques employing the measurements at two- or multi-ends of the line have been proposed in [8-15]. Unsynchronized measurements are utilized for estimating the fault location and the unsynchronization angle between the measurements at the two terminals of the line [8-10]. A lumped line model is used in [8] where the shunt capacitance for long lines is compensated in an iterative way. Reference [9] is also based on the lumped model and the shunt capacitance of the line is neglected. The technique presented in [10] first obtains the unsynchronization angle by solving a quadratic equation and then derives the fault location, ignoring the distributed parameter effects while considering the shunt admittance of the line. Synchronized measurements have been utilized in [11-15]. Reference [11] formulates the fault location problem based on the travelling wave equations considering losses. The ABCD parameters of the line is utilized in [13] for deriving the fault location based on the lumped line model. Synchronized voltage measurements from multi-ends of the lines are utilized to find the fault location assuming that the source impedances are known without considering the shunt capacitance in [14]. A method based on the fault generated transients and the travelling wave theory is presented in [15].

In this paper a new two-terminal synchronized sampling numerical algorithm for the analysis of single line to ground faults on short overhead transmission lines is presented. Background describing developments in synchronized sampling technology and previous algorithm developments are discussed in Section 2. Information about the previous work is given in Section 3. The transmission line modelling and related algorithm development is presented in Section 4. The new algorithm itself is presented in Section 5, where as the algorithm test results and conclusions are given in Section 6.

1530-1605/11 $26.00 © 2011 IEEE

2. Background

Recent advances in Information and Communications Technology (ICT) have led to significant developments in the use of intelligent systems for power system monitoring, control and protection. Supported by the Global Positioning System (GPS), Synchronised Measurement Technology (SMT) is fast becoming a key technology in this area. Its main components are: Synchronised/Phasor Measurement Units (SMU/PMU), Data Concentrators (DC), application software (AS) and its supporting communication networks (CN). In Fig. 1 a typical Wide Area Monitoring, Protection and Control (WAMPAC) architecture based on SMT is presented.

Fig. 1 illustrates how phasor/sample information is collected. In Fig. 1, phasor/sample information (and other electrical and non-electrical variables) is collected from the network by PMUs and forwarded over different communication media to the DCs. Two DCs forward selected information to the "Super DC", which is connected to the Real Time Monitoring centre. Selected WAMPAC applications can be run directly at this (top) level, along with the Data Archiving.

The objective of this paper is to propose a new numerical algorithm for analysis of faults on transmission lines based on SMT and synchronised sampling.

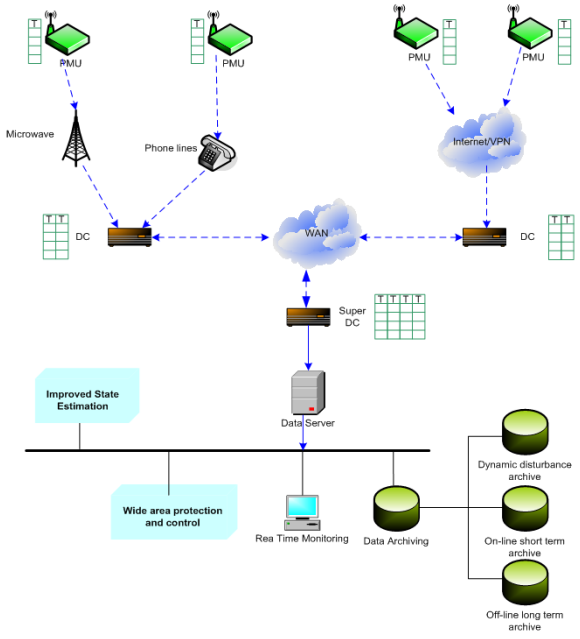

Fig. 1: Generic architecture of WAMPAC system.

3. Previous work

Previous efforts were aimed at implementing accurate fault location algorithms for short lines represented with lumped parameters and long lines represented with distributed parameters [1]

For short lines, the fault location is calculated directly using minimum square estimate method, as follows [1]:

$$x = \frac{-\sum_{m=a,b,c}\sum_{k=1}^{N} A_m(k)B_m(k)}{\sum_{m=a,b,c}\sum_{k=1}^{N} B_m^2(k)} \tag{1}$$

where

$$A_m(k) = \upsilon_{mS}(k) - \upsilon_{mR}(k) - d\sum_{p=a,b,c}[(r_{mp} + \frac{l_{mp}}{\Delta t})i_{pS}(k) - \frac{l_{mp}}{\Delta t} i_{pS}(k-1)] \quad m=\text{a,b,c} \tag{2}$$

$$B_m(k) = \sum_{p=a,b,c}\{(r_{mp} + \frac{l_{mp}}{\Delta t})[i_{pS}(k) + i_{pR}(k)] - \frac{l_{mp}}{\Delta t}[i_{pS}(k-1) + i_{pR}(k-1)]\} \quad m=\text{a,b,c} \tag{3}$$

where k is the sample point, Δt is sample period, subscripts S, R stand for the values from sending end and receiving end of the line.

For long lines, according to Bergeron's equations, the voltage and current profiles along the line are expressed as follows [11]:

$$\upsilon_{j,k} = \tfrac{1}{2}[\upsilon_{j-1,k-1} + \upsilon_{j-1,k+1}] + \frac{Z_c}{2}[i_{j-1,k-1} + i_{j-1,k+1}] + \frac{R\Delta x}{4}[i_{j-1,k-1} + i_{j-1,k+1}] - \frac{R\Delta x}{2} i_{j,k} \tag{4}$$

$$i_{j,k} = \frac{1}{2Z_c}[\upsilon_{j-1,k-1} - \upsilon_{j-1,k+1}] + \frac{1}{2}[i_{j-1,k-1} + i_{j-1,k+1}] + \frac{R\Delta x}{4Z_c}[i_{j-1,k+1} + i_{j-1,k-1}] \tag{5}$$

where $\Delta x = \frac{\Delta t}{\sqrt{lc}}$ is the distance that the wave travels with a sampling period Δt ; $Z_c = \sqrt{\frac{l}{c}}$ is the surge impedance.

Subscript j is the position expressed as a discrete point on the line and k is the sample point. The final location is obtained by an indirect method presented in [11]. The impact of parallel lines on the fault location has been taken into account in [11]

Methods presented in [1],[11] gave a sound base for extending the strategy of using the synchronized sampling approach by modelling the fault location more realistically and opening by this quite a new options for a detailed fault analysis. The assumption that faults are just pure metallic (bolted) faults is not always valid, particularly during arcing faults, or faults including fault resistance. In the next Section of the paper this issue will be addressed. New opportunities for establishing methods for a detailed fault analysis, e.g. including a detection of the nature of the faults ,i.e. arcing (transient) or non-arcing (permanent) faults, which is another important aspect of fault location process, will be shown.

4. Modelling of faulty transmission lines

The simplest approach to fault modelling is to model the fault as a pure metallic (bolted) fault. Statistically, faults are predominantly arcing faults; approximately 80% of all faults are followed by an arc, which contributes to the resistive component of the fault impedance. The fault path also includes the tower footing resistance and any other resistance at the fault point. An accurate fault location algorithm must consider all resistance components: the arc and the tower footing resistance, which are connected in series.

Fig. 2 shows a three-phase representation of a single line to ground arcing fault on a transmission line. It is assumed that current and voltage measurements are synchronously acquired at both line terminals and transmitted to the central Intelligent Electronic Device (IED) where they are processed by an appropriate numerical algorithm to determine the fault distance, l, arc voltage amplitude, U_a, and the tower footing resistance, R_F. A potential limitation of such an approach might be some unexpected problems with the synchronisation. It is assumed that the synchronisation is ideal, otherwise, some errors in fault analysis would be identified.

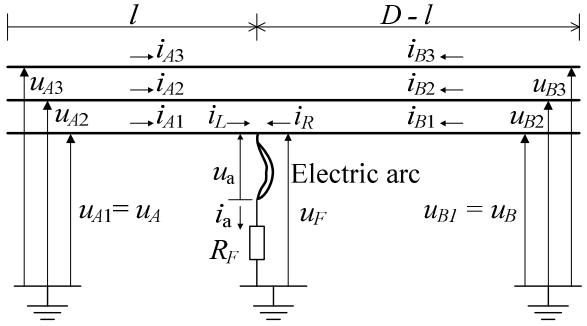

Fig. 2: Three-phase representation of the faulted line.

The fault arc has a highly nonlinear nature, causing distortions in the voltage and current waveforms along the transmission line. The arc voltage waveform can be modelled as a pure square wave [16-17]:

$$u_a(t) = U_a \operatorname{sgn}(i_a) \tag{6}$$

This practical arc voltage model is used to further develop the new numerical algorithm. Model (6) has just one unknown model parameter: the arc voltage amplitude U_a. Other arc models include a number of different parameters, but it will be shown that model (6) is accurate enough for developing new algorithms for overhead lines protection.

Using the symmetrical components approach, the left line terminal voltage u_A can be expressed as follows:

$$u_A = R_A^P\left(i_L + K_R i_L^0\right) + L_A^P\left(\frac{di_L}{dt} + K_L\frac{di_L^0}{dt}\right) + u_F \tag{7}$$

where R_A^P, R_A^0, L_A^P and L_A^0 are positive and zero sequence line resistance and inductance, respectively, i_L and i_L^0 are left line terminal current and its zero sequence component during the fault, u_F is fault voltage, and $K_R = \left(R_A^0 - R_A^P\right)/R_A^P$ and $K_L = \left(L_A^0 - L_A^P\right)/L_A^P$ are the compensation coefficients to account for the zero-sequence current flowing through the line. These coefficients can be calculated in advance and they remain constant.

The fault current i_a is the sum of the currents flowing to the fault from both of the line terminals (see Fig. 2):

$$i_a = i_L + i_R \tag{8}$$

Also, the fault voltage u_F can be expressed as:

$$u_F = U_a \operatorname{sgn}(i_a) + R_F i_a \tag{9}$$

Substituting equations (8) and (9) into equation (7) gives:

$$u_A = R_A^P\left(i_L + K_R i_L^0\right) + L_A^P\left(\frac{di_L}{dt} + K_L\frac{di_L^0}{dt}\right) + U_a \operatorname{sgn}(i_L + i_R) + R_F(i_L + i_R) \tag{10}$$

The line parameters can be expressed as products of the line length and per unit length values. Equation (10) then becomes:

$$u_A = r^P\left(i_L + K_R i_L^0\right)\cdot l + l^P\left(\frac{di_L}{dt} + K_L\frac{di_L^0}{dt}\right)\cdot l + \operatorname{sgn}(i_L + i_R)\cdot U_a + (i_L + i_R)\cdot R_F \tag{11}$$

where: l is the unknown distance from the left line terminal to the fault location, U_a is the unknown arc voltage magnitude and R_F is the unknown fault resistance. Equation (11) can then be rewritten in the following simplified form:

$$u_A = a_1 \cdot l + a_2 \cdot U_a + a_3 \cdot R_F \tag{12}$$

Coefficients a_1, a_2 and a_3 can be identified from equation (11):

$$a_1 = r^P\left[i_L + K_R i_L^0\right] + l^P\left(\frac{di_L}{dt} + K_L \frac{di_L^0}{dt}\right) \tag{13}$$

$$a_2 = \operatorname{sgn}\left[i_L + i_R\right] = \operatorname{sgn} i_a \tag{14}$$

$$a_3 = i_L + i_R = i_a \tag{15}$$

In equation (12) a_1, a_2, a_3 and u_A can be measured at both line terminals. The unknown parameters can be arranged in the vector **x**, as follows:

$$\mathbf{x} = \left[l \quad U_a \quad R_F\right]^T \tag{16}$$

where "T" denotes matrix transposition.

Thus, the generic parameter model of the problem can be expressed as follows:

$$u_A = \left[a_1 \quad a_2 \quad a_3\right] \cdot \left[l \quad U_a \quad R_F\right]^T = \mathbf{a}\,\mathbf{x}^{\mathrm{T}} \tag{17}$$

where a is a 1×3 coefficient model matrix. Finally, to take into account the uncertainties in the process analysed, random noise, μ, should be added to (17) (this noise has normal distribution with mathematical expectation equal to 0):

$$u_A = \mathbf{a}\,\mathbf{x}^{\mathrm{T}} + \mu \tag{18}$$

Expression (18) is the generic mathematical model of the measured voltage on the faulted phase. This is the starting point for designing a suitable technique for estimating the fault distance, arc voltage amplitude and tower footing resistance. Since the model is linear, linear parameter estimation techniques can be implemented here. The model order, as defined by the number of unknown model parameters, is 3, so the option of applying a non-recursive estimator is acceptable for future real-time processing. This will be shown in the next Section of the paper, in which the application of a non-recursive Least Error Squares estimation method is presented.

For the calculation of the first order derivatives of currents, the polynomial interpolation approach was used.

5. Least error squares parameter estimation

If the input signals are uniformly sampled with the sampling frequency f_s, then discrete presentation of time, having index m is given by $t = t_m = mT_s$. Assuming that N samples, which belong to a data window of size T_{dw}, are simultaneously processed, then a suitable equation (18) can be written for each time step within the data window. In this way, N equations will be obtained for N samples. These can be presented in the following clear matrix form:

- measurement vector of voltage samples:

$$\mathbf{u_A} = \left[u_A(t_1) \quad \cdots \quad u_A(t_N)\right]^{\mathrm{T}} = \left[u_{A1} \quad \cdots \quad u_{AN}\right]^{\mathrm{T}} \tag{19}$$

- coefficients of suitable model matrices:

$$\mathbf{a_1} = \begin{bmatrix} r^P\left[i_L + K_R i_L^0\right] + l^P\left(\frac{di_L}{dt} + K_L \frac{di_L^0}{dt}\right)\Big|_{(t=t_1)} \\ \vdots \\ r^P\left[i_L + K_R i_L^0\right] + l^P\left(\frac{di_L}{dt} + K_L \frac{di_L^0}{dt}\right)\Big|_{(t=t_N)} \end{bmatrix} \tag{20}$$

$$\mathbf{a_2} = \left[\operatorname{sgn}\left[i_L + i_R\right]\Big|_{(t=t_1)} \quad \cdots \quad \operatorname{sgn}\left[i_L + i_R\right]\Big|_{(t=t_N)}\right]^{\mathrm{T}} \tag{21}$$

$$\mathbf{a_3} = \left[i_L + i_R\Big|_{(t=t_1)} \quad \cdots \quad i_L + i_R\Big|_{(t=t_N)}\right]^{\mathrm{T}} \tag{22}$$

For a given data window, the following holds:

$$\mathbf{u_A} = \left[\mathbf{a_1} \quad \mathbf{a_2} \quad \mathbf{a_3}\right] \cdot \mathbf{x}^{\mathrm{T}} + \boldsymbol{\mu} = \mathbf{A}\,\mathbf{x}^{\mathrm{T}} + \boldsymbol{\mu} \tag{23}$$

where **A** is a coefficient model matrix. The optimal parameter estimates are obtained by using the Least Error Squares (LES) estimation method:

$$\mathbf{x} = \left(\mathbf{A}^{\mathrm{T}}\mathbf{A}\right)^{-1}\mathbf{A}^{\mathrm{T}}\mathbf{u}_{\mathbf{A}} \qquad (24)$$

where $\left(\mathbf{A}^{\mathrm{T}}\mathbf{A}\right)^{-1}\mathbf{A}^{\mathrm{T}}$ is the *left pseudo-inverse matrix* of the model matrix **A**. The model order n (here $n = 3$) is determined by the number of unknowns. The inversion of a 3x3 matrix is a trivial task, even for ordinary hardware platforms, so the algorithm could be implemented in future IEDs.

In the above algorithm, the accuracy of classical fault locators has been significantly improved by taking the arc voltage into consideration. Furthermore, the new algorithm provides a means of detecting arcing faults to aid adaptive auto-reclosure.

In the algorithm derivation, the capacitive nature of the line was neglected, so the presented solution can be applied to "short" lines (lines of length less than 100 km).

The difference between this algorithm and the present state of the art is that, due to the algorithm being derived in the time domain, it is able to estimate the fault resistance and indicate the presence of a fault arc as well as estimating the fault distance. The effects of the fault arc on the accuracy of the algorithm are assessed; the algorithm is rigorously tested for varying arc voltage waveform shapes and arc elongation effects. As the algorithm was derived in the time domain, it has a faster convergence time than those derived in the spectral domain. The algorithm is based on synchronised data sampling at both line terminals.

6. Algorithm testing

The algorithm performance was investigated by simulating different kinds of faults on a 100 km long overhead transmission line. In Appendix I the single line diagram of the simulated line and its parameters are given.

Single line-to-ground arcing and arcless faults were simulated at different locations along the line. In each case the fault inception time was set at $t = 23$ ms and the tower footing resistance R_F was varied in the range of 0-100 Ω. It was assumed that the line was loaded before the fault inception. The sampling frequency was $f_s = 3200$ Hz. The data window size was $T_{dw} = 40$ ms ($N = 128$ samples per data window). The selection of the above parameters are typical when testing algorithms for fault location/analysis.

Faults at 10 km, 50 km, and 90 km from the left line terminal, both with and without arcs, will be presented. The algorithm was rigorously tested using the following criteria: a) comparison between one- and two-port algorithms and b) assessment of the suitability of the proposed algorithm for adaptive autoreclosure.

6.1. Comparison between one- and two-port algorithms

The accuracy of the proposed algorithm is compared with that of a corresponding algorithm using single line terminal data. A 90 km arcing fault is used to demonstrate the features of the two-port algorithm. The ATP simulated voltages and currents from both line terminals are to estimate the unknown model parameters of (16). In Figs. 5 and 6 the simulated currents and voltages from the left line terminal are presented, respectively. These input data and those from the right line terminal contain the information about the unknown parameters being estimated by the proposed algorithm.

From Fig. 7, it is obvious that the new two-port algorithm gives a more accurate estimation of the distance fault. From Fig. 8, it can be concluded that the one port algorithm does not reach a stable estimate of the arc voltage amplitude; it cannot, therefore, be used as a reliable criterion for controlling the auto-reclosure. It is assumed that the auto-reclosure would be blocked if the arc is not detected at the fault location; the arc voltage amplitude is used to indicate the presence of an arc). From the above test it can be concluded that two-port algorithms offer a higher accuracy and greater potential for different applications. Adaptive auto-reclosure issues are explored in the next Subsection.

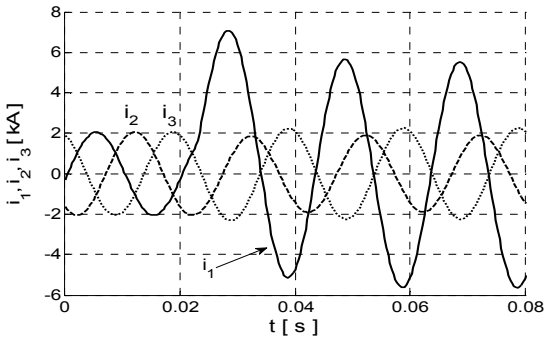

Fig. 5: Simulated left line terminal currents.

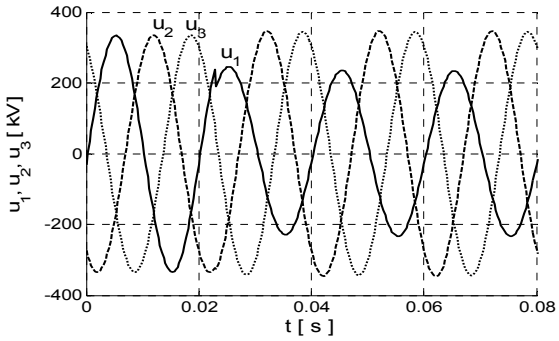

Fig. 6: Simulated left line terminal voltages.

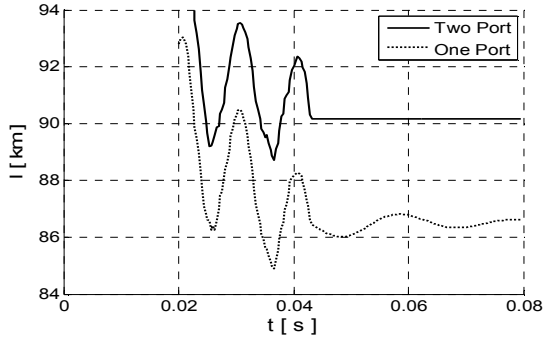

Fig. 7: Estimated fault distance.

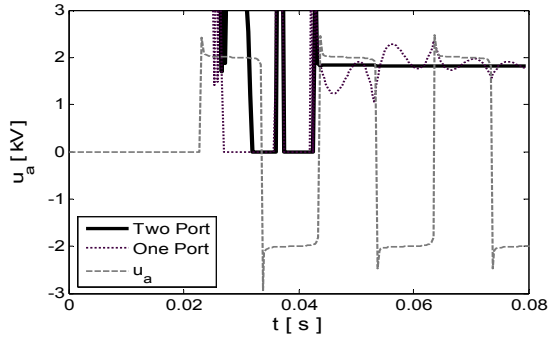

Fig. 8: Estimated arc voltage magnitude.

6.2. Fault nature detection

If the arc model includes the arc voltage, the above algorithm can be used to ascertain the nature of the fault. By evaluating the estimated arc voltage amplitude it is possible to distinguish between arcing (transient) and non-arcing (permanent) faults. In this test, an additional arc phenomenon is included: *arc elongation*. It was assumed that the arc elongated at a rate of 12 m/s – as obtained from the analysis of a real arc. In Fig. 9 the elongated arc voltage u_a, its estimated amplitude, and the control signal indicating that the fault is transient are presented. The excellent tracking abilities of the algorithm are obvious. The auto-reclosure control signal "*C*" has a true (logical 1) value, so the auto-reclosure is released; conversely, for an arcless fault, it has a false (logical 0) value, so the auto-reclosure is blocked.

Simultaneously to the arc voltage amplitude, the unknown fault distance (90 km) and tower footing resistance R_F (30 Ω) are estimated (see Figs. 10 and 11). The equivalent tests were carried out for other fault locations on the line, and resistances R_F. In each case the algorithm has given accurate results.

For the equivalent test but without an arc, the algorithm detects the arcless fault, as presented in Fig. 12. Here the estimated arc voltage amplitude is zero. Consequently, the auto-reclosure control signal is false. In [17], more details about the concept of adaptive auto-reclosure are given.

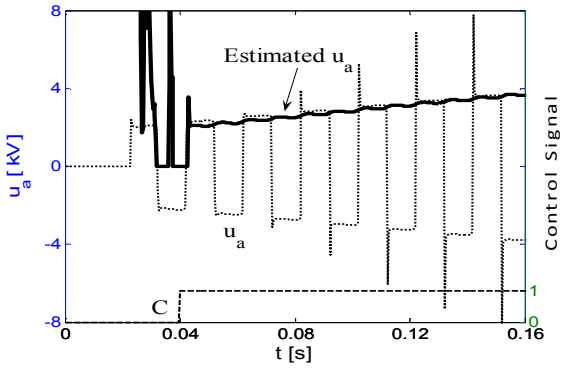

Fig. 9: Estimated arc voltage magnitude for a 90 km arcing fault.

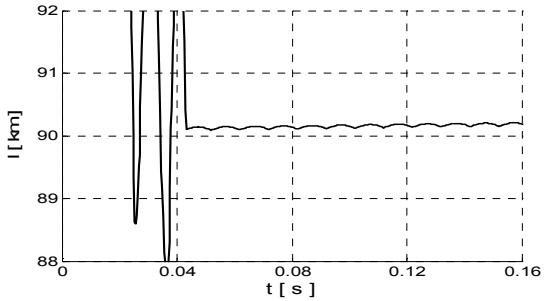

Fig. 10: Estimated fault distance for a 90 km arcing fault.

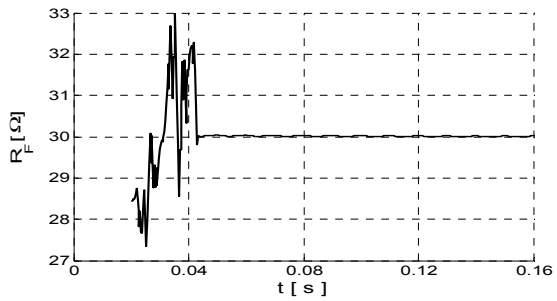

Fig. 11: Estimated fault resistance.

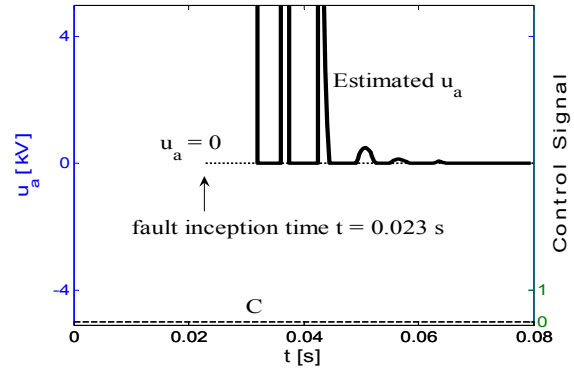

Fig. 12: Estimated arc voltage magnitude for a 90 km arcless fault.

6.3. Sensitivity to synchronisation errors

The above results were presented under the assumption that the relays at the two line terminals were perfectly synchronised. In this Subsection the sensitivity of the algorithm to synchronisation errors is investigated. For this, an arcing fault was simulated at 10 km from the left line terminal. The arc voltage amplitude was $U_a = 2$ kV, and fault resistance R_F was 10 Ω. The first row of Table I shows the level of synchronisation error, expressed as angle θ in degrees. The steady-state error in the estimation of each unknown parameter is presented. Obviously, a very high level of accuracy has been achieved.

TABLE I: SENSITIVITY TO SYNCHRONISATION ERRORS.

θ	6°	12°	18°	24°
Err I_f (%)	0.6573	1.2606	1.8433	2.403
Err u_a (%)	0.0098	0.0102	0.0103	0.01
Err R_f (%)	0.8093	1.7376	2.9195	4.3614

7. Conclusions

In this paper a new time domain adaptive estimation numerical algorithm for the analysis of single line to ground faults on short overhead transmission lines, based on synchronized phasors technology and the implementation of parameter estimation theory, has been presented. It was derived based on some earlier work by the authors briefly described in the paper. It has been demonstrated that the accuracy of fault locators can be significantly improved by realistically modelling the arcing fault. It was shown that the fault nature (permanent metallic or transient arcing) can be efficiently determined. The importance of fault arc modelling was investigated and it was proved that realistic arc modelling can improve the quality of fault locators and algorithms for the analysis of faults on transmission lines. The proposed solutions is limited to short transmission lines, so the algorithm for fault location, developed in the earlier research by the authors, is still a superior solution for long lines.

8. References

[1] M. Kezunovic and B. Perunicic, "Fault Location," Wiley Encyclopedia of Electrical and Electronics Terminology, Vol. 7, pp 276-285, John Wiley, 1999.

[2] K. Takagi, Y. Yomakoshi, M. Yamaura, R. Kondow, and T. Matsushima, "Development of a new type fault locator using the one-terminal voltage and current data", IEEE Transactions on Power Apparatus and System, Vol. 101, No. 8, August 1982, pp. 2892-2898.

[3] L. Eriksson, M.M. Saha, and G.D. Rockefeller, "An accurate fault locator with compensation for apparent reactance in the fault resistance resulting from remote-end infeed", IEEE Transactions on Power Apparatus and Systems, Vol. PAS-104, No.2, February 1985, pp. 424-436.

[4] Q. Zhang, Y. Zhang, W. Song, and D. Fang, "Transmission line fault location for single-phase-to-earth fault on non-direct-ground neutral system", IEEE Transactions on Power Delivery, Vol. 13, No.4, October 1998, pp. 1086-1092.

[5] Q. Zhang, Y. Zhang, W. Song, and Y. Yu, "Transmission line fault location for phase-to-earth fault using one-terminal data", IEE Proceedings- Generation, Transmission and Distribution, Vol. 146, No. 2, March 1999, pp. 121-124.

[6] J. Izykowski, E. Rosolowski, and M. M. Saha, "Locating faults in parallel transmission lines under availability of complete measurements at one end", IEE Proceedings-

Generation, Transmission and Distribution, Vol. 151, No. 2, March 2, 2004, pp. 268 – 273.

[7] M. Djuric, Z. Radojevic, and V. Terzija, "Distance protection and fault location utilizing only phase current phasors", IEEE Transactions on Power Delivery, Vol. 13, No. 4, October 1998, pp. 1020-1026.

[8] Novosel, D. G. Hart, E. Udren, and J. Garitty, "Unsynchronized two-terminal fault location estimation", IEEE Transactions on Power Delivery, Vol. 11, No. 1, January 1996, pp. 130-138.

[9] A.A. Girgis, D. G. Hart, and W.L. Peterson, "A new fault location technique for two-and three-terminal lines", IEEE Transactions on Power Delivery, Vol. 7, No. 1, January 1992, pp. 98-107.

[10] M. Sachdev and R. Agarwal, "A technique for estimating transmission line fault locations from digital impedance relay measurements", IEEE Transactions on Power Delivery, Vol. 3, No. 1, January 1998, pp. 121-129.

[11] A. Gopalakrishnan, M. Kezunovic, S.M. McKenna, and D.M. Hamai, "Fault location using distributed parameter transmission line model", IEEE Transactions on Power Delivery, Vol. 15, No. 4, October 2000, pp. 1169-1174.

[12] Y. H. Lin, C. W. Liu, and C. S. Chen, "A new PMU-based fault detection/location technique for transmission lines with consideration of arcing fault discrimination – part I: theory and algorithms", IEEE Transactions on power delivery, Vol. 19, No. 4, October 2004, pp. 1587-1593.

[13] D. J. Lawrence, L. Cabeza, and L. Hochberg, "Development of an advanced transmission line fault location system, Part I-Input transducer analysis and requirements, Part II-Algorithm development and simulation", IEEE Transactions on Power Delivery, Vol. 7, No. 4, October 1992, pp. 1963-1983.

[14] S.M. Brahma, "Fault location scheme for a multi-terminal transmission line using synchronized voltage measurements", IEEE Transactions on Power Delivery, Vol. 20, No. 2, April 2005, pp. 1325 – 1331.

[15] F. H. Magnago and A. Abur, "Accurate fault location using wavelets", IEEE Transactions on Power Delivery, Vol. 13, No. 4, December 1998, pp. 1475-1480.

[16] Terzija V, Nelles D, "Parametrische Modelle des Lichtbogens und Parameterschätzung auf Grund der simulierten und echten Daten," (in German) TB 183/93, Univ. Kaiserslautern, Kaiserslautern, Germany, July 1993.

[17] M. Djuric, V. Terzija, "A new approach to the arcing faults detection for autoreclosure in transmission systems," IEEE Trans. on Power Delivery, Vol. 10, No 4, Oct. 1995, pp. 1793-1798

9. Appendix

In Fig. 13, the schematic diagram of a 400kV, 100km long, overhead transmission line is presented. In Tables II and III, the parameters of networks A and B and the line parameters are listed, respectively.

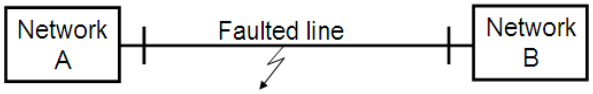

Fig. 13: Single line diagram of the simulated faulted line.

TABLE II: PARAMETERS OF NETWORKS A AND B.

Parameters	Networks	
	A	**B**
$U_{LL,RMS}$ [kV]	416	400
φ_1 [^{0}]	0	-20
R [Ω]	1.0185892	0.6366183
L [H]	0.0509295	0.0318309
R_0 Ω	2.0371785	1.2732366
L_0 H	0.1018589	0.0636618

TABLE III: LINE PARAMETERS.

Parameter	*p*- and *n*-sequence	0-sequence
Resistance, Ω/km	0.065	0.195
Inductance mH/km	0.95493	2.86479